PHYSICAL REVIEW B **67**, 035208 (2003)

Dicarbon defects in carbon-doped GaAs

K. H. Tan, S. F. Yoon, Q. F. Huang, R. Zhang, and Z. Z. Sun
School of Electrical and Electronic Engineering (Block S1), Nanyang Technological University, Nanyang Avenue, 639798 Singapore

J. Jiang, W. Feng, and L. H. Lee
MBE Technology Pte Limited, 14 Science Park Drive, #02-04A The Maxwell, Singapore Science Park, 118226 Singapore

(Received 16 July 2002; revised manuscript received 2 October 2002; published 30 January 2003)

Carbon-doped GaAs (GaAs:C) samples have been grown using the solid source molecular-beam epitaxy system and carbon tetrabromide (CBr_4) as the carbon-doping source. For the purpose of investigation, a relatively high substrate temperature of 650 °C was used to induce the formation of dicarbon defects in selected samples. Hall effect, secondary-ion mass spectroscopy (SIMS), and x-ray-diffraction (XRD) measurements have been used for sample characterization. Using data from Hall effect and SIMS measurements, calculations on the lattice mismatch induced by several possible structures of the dicarbon defect were carried out. A comparison between calculated results and lattice mismatch measured by XRD suggests the dicarbon defects in compensated GaAs:C samples exist mainly as deep donors and are oriented along the $\langle 111 \rangle$ crystal direction.

DOI: 10.1103/PhysRevB.67.035208 PACS number(s): 61.72.Vv, 61.72.Ji

I. INTRODUCTION

GaAs-based heterojunction bipolar transistors (HBT's) have attracted wide interest for high-speed application due to their superior electron mobility compared to silicon-based devices. To improve the high-speed performance of GaAs-based HBT's, or in other words, to increase the cutoff frequency f_T and maximum frequency of oscillation $f_{\max}$ of the device, it is desirable to reduce the resistance of the device base layer. The use of carbon as a *p*-type dopant in GaAs enables the device base layer hole concentration to exceed 10^{20} cm^{-3}. Such a high doping level would reduce the base layer resistance significantly. Furthermore, the low diffusion coefficient of the carbon dopant in GaAs, compared to other *p*-type dopants, such as Be and Zn,[1] would minimize the outward diffusion of dopant from the base layer, and hence provide better control of the base layer resistance given a certain thickness. The low diffusion coefficient of carbon also enables the formation of an abrupt base-emitter and base-collector junction, thus enhancing the dc performance of the HBT.

For carbon-doping levels in GaAs higher than 10^{20} cm^{-3}, post growth annealing or growth above 650 °C will reduce its Hall carrier concentration but the total carbon concentration remains unchanged.[2,3] This reduction in carrier concentration is observed to occur concurrently following decrease in lattice contraction caused by the substitutional carbon atom C_{As}. It is suggested that the reduction in Hall carrier concentration is due to the passivation of C_{As} by an interstitial hydrogen atom.[4–6] During annealing or high-temperature growth, these interstitial hydrogen atoms diffuse and react with the C_{As} to form C-H bonds on the arsenic sites. These C-H pairs have a larger lattice parameter than C_{As} and will reduce the lattice contraction in the GaAs:C. However, a similar observation of reduction in carrier concentration was made on GaAs:C annealed or grown at high temperature by chemical beam epitaxy[7] and solid source molecular-beam epitaxy (SSMBE).[3] Since the SSMBE technique is known to have negligible hydrogen content in the chamber, the passivation of C_{As} by hydrogen atoms alone may not be adequate to explain the reduction in carrier concentration.

A split-interstitial C-C pair (dicarbon defect) was used to explain the concurrent reduction in carrier concentration and increase in the lattice parameter.[8] The dicarbon defect is formed through moving an interstitial carbon atom, which is then captured by the C_{As}. The existence of this defect in GaAs:C samples was first demonstrated experimentally by Wagner *et al.*[9] from Raman-scattering measurements, which showed two peaks at 1742 and 1859 cm^{-1}, respectively. Although it was revealed that dicarbon defects are responsible for the observed peaks, its detailed structure remains unclear. Three structures were proposed for the dicarbon defect: (i) [100]-split-interstitial $(CC)^+$, proposed by Cheong and Chang,[8] (ii) [110]-split-interstitial $(CC)^+$, and (iii) [111]-split-interstitial $(CC)^+$, both of which were proposed by Davidson *et al.*[10] using comparison between the Raman peaks and *ab initio* calculation.

This paper presents an investigation of the structure of dicarbon defects in GaAs:C by making use of measurements from x-ray diffraction (XRD), secondary-ion mass spectroscopy (SIMS), and Hall effect. GaAs:C samples were grown using SSMBE and carbon tetrabromide (CBr_4) as a *p*-type carbon source. Due to the fact that the three proposed structures of dicarbon defect have different orientations in the GaAs crystal, a distinguishable effect on the lattice parameter will be induced. By comparing the experimental and theoretical value of the lattice parameter for these dicarbon defect structures, the predominant dicarbon defect structure in compensated GaAs:C can be determined.

II. EXPERIMENTAL PROCEDURE

Six GaAs:C samples have been grown on a GaAs (001) substrate using the SSMBE system. The CBr_4 was used as the carbon source and contained in a sealed stainless-steel cylinder. The source was sublimed between 2 °C and 20 °C to provide the desired CBr_4 flux, ranging from 2×10^{-8} to 2×10^{-7} Torr. No carrier gas was used and the flux magni-

 ©2003 The American Physical Society

TABLE I. Experimental results of Hall effect, lattice mismatch, and carbon density from SIMS measurement [C].

Sample	[C] (cm^{-3})	Hall concentration (cm^{-3}) ±10%	Lattice mismatch (ppm) ±50
1	3.2×10^{19}	3.2×10^{19}	−450
2	3.2×10^{19}	1.0×10^{19}	≃160
3	1.1×10^{20}	1.1×10^{20}	−1609
4	1.1×10^{20}	5.9×10^{19}	−834
5[a]	1.5×10^{20}	1.2×10^{20}	−1650
6[a]	1.5×10^{20}	5.5×10^{19}	−850
7	1.6×10^{20}	1.6×10^{20}	−2311
8	1.6×10^{20}	8.9×10^{19}	−1266

[a]The experimental data are from samples grown by metal-organic vapor-phase epitaxy (MOVPE) reported by Hanna and Mayerfeld (Ref. 2).

tude was regulated by a precision leak valve. The CBr_4 cylinder was connected to the molecular-beam epitaxy MBE chamber by a gas line, which was heated up to 80 °C to prevent condensation of CBr_4 along the gas line. In our experiment, the thickness of all samples was maintained at 0.23 μm.

One advantage of using CBr_4 as the dopant source in GaAs is the high electrical activation of the carbon atoms. Within a growth temperature range of 560 °C–600 °C, GaAs:C grown using CBr_4 as the dopant source exhibits almost 100% electrical activation[11] of the carbon atoms even for concentrations of up to $2\times10^{20}\ \mathrm{cm}^{-3}$. However, for GaAs:C samples grown above 650 °C the Hall carrier concentration is compensated and dicarbon defects are formed, while the total carbon concentration [C] remains unchanged.[3] The dependence of C_{As} or the dicarbon defect and the independence of [C] on growth temperature enable the growth of GaAs:C samples with different C_{As} concentrations and essentially identical [C]. In order to show the effect of dicarbon defect on lattice parameter, it is our intention, therefore, to prepare the samples in pairs. Each pair comprises a sample with all carbon atoms as C_{As}, and another sample containing dicarbon defects (details will be discussed in the theoretical section). Thus, three pairs of samples were grown at a CBr_4 flux of 1×10^{-7}, 2×10^{-7}, and 2×10^{-8} Torr, respectively. For each pair, one sample was grown at 600 °C and the other at 650 °C, respectively.

The samples were characterized using Hall effect, SIMS, and XRD measurements. The Hall-effect measurements were carried out at room temperature. For XRD measurements, a normal (004) scan was performed to determine the lattice mismatch in the growth direction $(\Delta a/a)_\perp$, while the asymmetric x-ray reflection was measured by scanning the sample in the (115) and $(\bar{1}\bar{1}5)$ planes. The asymmetric x-ray reflection gives information about the lattice mismatch perpendicular[12] to the growth direction $(\Delta a/a)_\parallel$, which is used to determine the degree of strain in the samples. The $(\Delta a/a)_\parallel$ values of our samples were around ±50 ppm, which was well within measurement error, and hence can be neglected. Thus, all samples in our experiment can be regarded as fully strained. The results of SIMS, Hall effect, and XRD measurements are shown in Table I. Samples 5 and 6 were annealed above 700 °C, and were reported by Hanna and Majerfeld.[2]

III. THEORETICAL CONSIDERATIONS

In this section, the effect of various dicarbon defect structures on the lattice parameter will be calculated. In a pure GaAs crystal, the nearest distance between a gallium and arsenic atom d can be defined as

$$d=r_{Ga}+r_{As}, \tag{1}$$

where r_{Ga} and r_{As} are the radii of the gallium and arsenic atoms, respectively. In the case of GaAs:C, the nearest distance between a gallium and substitutional carbon atom (C_{As}), $d_{C_{As}}$ will be

$$d_{C_{As}}=r_{Ga}+r_C, \tag{2}$$

where r_C is the radius of the carbon atom.

However, for a crystal system where a pair of carbon atoms occupies an arsenic site, the calculation of the nearest distance between centers of the carbon atom pair to the gallium atom can be complicated. To do this, the approach used by Chen *et al.*[13] for the calculation of interstitial atom pairs is adopted.

A. [100]-split-interstitial $(CC)^+$ structure

The geometry of the [100]-split-interstitial $(CC)^+$ structure is shown in Fig. 1(a). It can be shown that

$$\begin{aligned} d_{(CC)^+100}&=\overline{OK}=\sqrt{3}\,\overline{OG}=\sqrt{3}(\overline{OA}+\overline{AG})\\ &=\frac{1}{\sqrt{3}}\overline{OA}+\sqrt{\overline{AK}^2-\frac{2}{3}\overline{OA}^2}. \end{aligned} \tag{3}$$

Because $\overline{OA}=r_C$ and $\overline{AK}=r_{Ga}+r_C$, the above equation can be written as

$$d_{(CC)^+100}=\frac{1}{\sqrt{3}}r_C+\sqrt{(r_C+r_{Ga})^2-\frac{2}{3}r_c^2}. \tag{4}$$

It can be seen that $d_{(CC)^+100}$ is identical to the d of the interstitial carbon atom pair, as reported by Chen *et al.*[13]

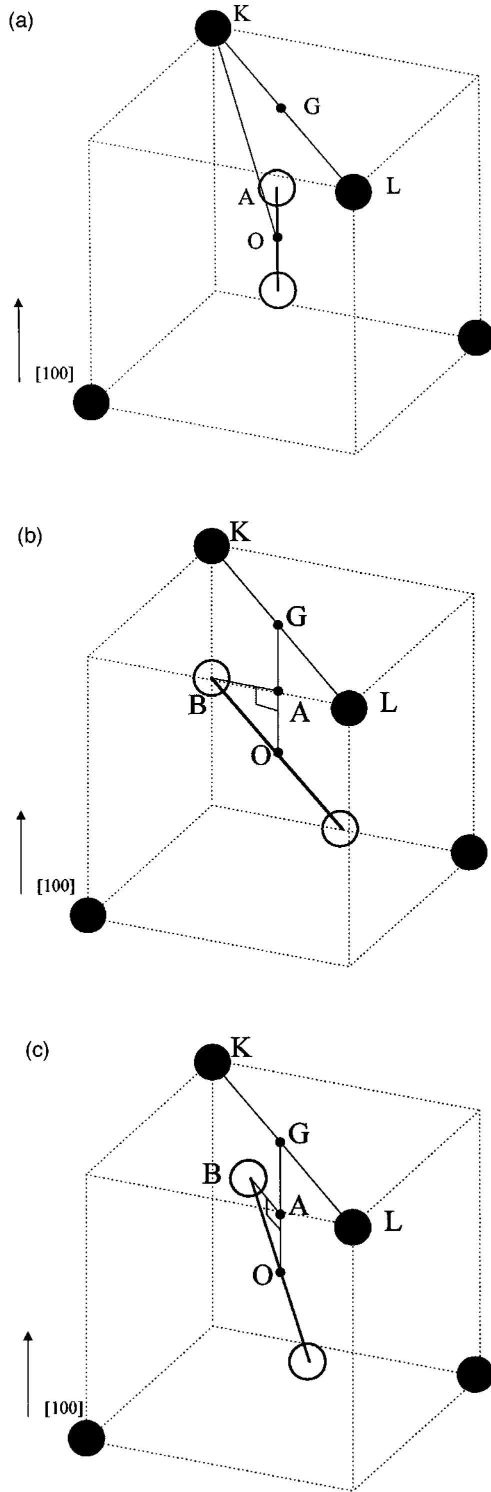

FIG. 1. Crystal structures for (a) [100]-split-interstitial $(\mathrm{CC})^+$, (b) [110]-split-interstitial $(\mathrm{CC})^+$, and (c) [111]-split-interstitial $(\mathrm{CC})^+$. Solid circles depict gallium atoms and open circles depict carbon atoms. G is the midpoint of $\overline{KL}$.

B. [110]-split-interstitial $(\mathrm{CC})^+$ structure

The geometry of the [110]-split-interstitial $(\mathrm{CC})^+$ structure is shown in Fig. 1(b). It can be shown that

$$d_{(\mathrm{CC})^+110}=\overline{OK}=\sqrt{3}\,\overline{OG}=\sqrt{3}(\overline{OA}+\overline{AG}), \tag{5}$$

$$\overline{AG}^2=\frac{\overline{BK}^2-\overline{OG}^2}{2}. \tag{6}$$

Solving Eqs. (5) and (6), it can be shown that

$$d_{(\mathrm{CC})^+110}=\frac{2}{\sqrt{3}}\overline{OA}+\sqrt{\overline{BK}^2-\frac{2}{3}\overline{OA}^2}, \tag{7}$$

where $\overline{OA}=r_{\mathrm{C}}/\sqrt{2}$ and $\overline{BK}=r_{\mathrm{C}}+r_{\mathrm{Ga}}$.

C. [111]-split-interstitial $(\mathrm{CC})^+$ structure

The geometry of the carbon atom pair in the [111]-split-interstitial $(\mathrm{CC})^+$ structure is shown in Fig. 1(c). Similarly, by formulating the value of $\overline{OK}$ in terms of r_{C} and r_{Ga}, it can be shown that

$$d_{(\mathrm{CC})^+111}=\overline{OK}=\sqrt{3}\,\overline{OG}=\sqrt{3}(\overline{OA}+\overline{AG})=\sqrt{3}\left(\overline{OA}+\frac{\overline{BK}}{\sqrt{3}}\right), \tag{8}$$

where $\overline{OA}=r_{\mathrm{C}}/\sqrt{3}$ and $\overline{BK}=r_{\mathrm{C}}+r_{\mathrm{Ga}}$. Equation (8) can be rewritten as

$$d_{(\mathrm{CC})^+111}=2r_{\mathrm{C}}+r_{\mathrm{Ga}}. \tag{9}$$

D. Lattice mismatch calculation

For an epitaxially grown GaAs:C layer, in which all the carbon atoms are electrically active and exist as $\mathrm{C_{As}}$, the lattice mismatch to the substrate $(\Delta a/a)_\perp$ is defined as[13]

$$\left(\frac{\Delta a}{a}\right)_\perp=\frac{c_{11}+2c_{12}}{c_{11}}\frac{d_{\mathrm{C_{As}}}-d}{d}\frac{N_c}{N_o}, \tag{10}$$

where c_{11} and c_{12} are the stiffness coefficients of the crystal. For GaAs, the value of c_{11} and c_{12} are 11.18×10^{11} and 5.38×10^{11} dyn/cm^2, respectively. N_c and N_o are the density of carbon atoms and arsenic atoms $(2.21\times10^{22}\ \mathrm{cm}^{-3})$, respectively. The $(c_{11}+2c_{12})/c_{11}$ term is included to account for the fully strained nature of the epitaxial layer in all our samples.

However, for an epitaxially grown GaAs:C layer in which the carbon atoms are partly present in the dicarbon defect state, its mismatch to the substrate layer $(\Delta a/a)_\perp$ is defined as

$$\left(\frac{\Delta a}{a}\right)_\perp=\frac{c_{11}+2c_{12}}{c_{11}}\frac{1}{dN_o}[N_{\mathrm{C_{As}}}(d_{\mathrm{C_{As}}}-d)+N_{\mathrm{CC}}(d'-d)], \tag{11}$$

where d' can be taken as $d_{(\mathrm{CC})^+100}$, $d_{(\mathrm{CC})^+110}$, or $d_{(\mathrm{CC})^+111}$, depending on the structure to be calculated. $N_{\mathrm{C_{As}}}$ and N_{CC} are the concentration of $\mathrm{C_{As}}$ and dicarbon defects, respectively. Due to the fact that the dicarbon defect behaves as a single deep level donor,[8] which compensates part of $N_{\mathrm{C_{As}}}$, the value of $N_{\mathrm{C_{As}}}$ can be calculated as follows:

$$N_{\mathrm{C_{As}}}=N_{\mathrm{Hall}}+N_{\mathrm{CC}}, \tag{12}$$

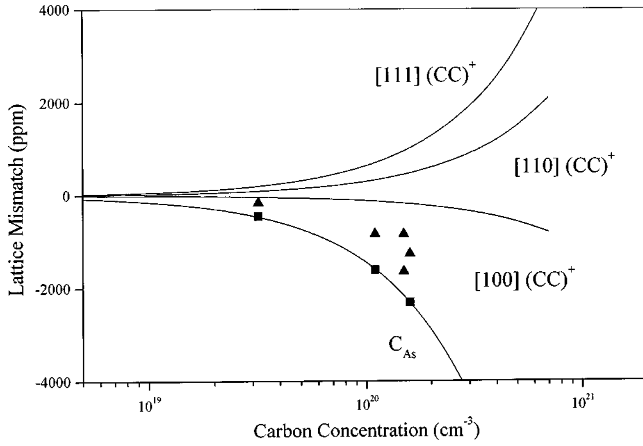

FIG. 2. Plot of lattice mismatch as function of carbon concentration for substitutional carbon atom C_{As}, [100]-split-interstitial $(CC)^+$, [110]-split-interstitial $(CC)^+$, and [111]-split-interstitial $(CC)^+$. Experimental data points for compensated GaAs:C samples are denoted by solid triangles, while experimental data points for noncompensated GaAs:C samples are denoted by solid squares.

where N_{Hall} is the Hall carrier concentration. N_{CC} can be related to $N_{C_{As}}$ as follows:

$$N_C = 2N_{CC} + N_{C_{As}}, \tag{13}$$

where N_C is the carbon atom concentration taken from SIMS measurement. By solving Eqs. (12) and (13), a unique value of $N_{C_{As}}$ and N_{CC} can be obtained. The lattice mismatch caused by different CC structures as a function of dicarbon defect concentration is shown in Fig. 2. In Table II, the calculated lattice mismatch caused by different dicarbon defect structures is compared to the experimental data for different samples.

It is noted that the effect of hydrogen-related bonds is not included in Eq. (11). This is because of the fact that samples grown by SSMBE are known to have negligible hydrogen content as mentioned earlier. Unlike metal-organic chemical-vapor deposition and metal-organic molecular-beam epitaxy (MOMBE), SSMBE uses sources, such as Ga, As_4, and CBr_4, which are highly free from hydrogen. The background hydrogen pressure in our SSMBE chamber measured by *in situ* quadrupole mass spectroscopy is $\sim 5\times 10^{-10}$ Torr. Such an insignificantly low hydrogen background pressure in the growth chamber would result in a negligible amount of hydrogen contamination in our samples. This is consistent with published reports,[14,15] which indicated a negligible hydrogen content from SIMS measurement (below detection limit) in SSMBE-grown samples. For hydrogen-related bonds to have a measurable effect on the lattice mismatch, their concentration must be greater than 10^{18} cm^{-3}. Furthermore, another report[16] has shown that SSMBE-grown GaAs:C samples do not exhibit any carbon-hydrogen-bond-related peaks from local vibration mode absorption spectroscopy measurement, as opposed to MOMBE- and MOVPE-grown samples, indicating negligible amounts of hydrogen-related bonds in the material.

IV. DISCUSSION

From Fig. 2, it can be seen that the $[100]$-$(CC)^+$ structure leads to a contraction of the GaAs lattice, while both the $[110]$-$(CC)^+$ and $[111]$-$(CC)^+$ structures lead to an expansion. However, the lattice parameter of these structures is larger than that of the substitutional carbon atom C_{As}. Thus, any compensation of the Hall carrier concentration, which is caused by the transformation from C_{As} to the dicarbon defect, may lead to reduction in the lattice contraction. From comparison between the experimental and calculated results shown in Table II, it can be concluded that the dicarbon defect structure in the GaAs:C epitaxial layer is dominated by the $[111]$-$(CC)^+$ structure. The calculated results of the $[111]$-$(CC)^+$ structure for all samples lie within 6% from the experimental data. This is well within the estimated error range of 10% in the experimental data. Although the results strongly suggest a predominance of the $[111]$-$(CC)^+$ structure in the compensated GaAs:C epitaxial layer, they do not rule out the existence of either the $[100]$-$(CC)^+$ or $[110]$-$(CC)^+$ structures in insignificant quantities.

TABLE II. Comparison of lattice mismatch between experimental results and theoretical calculation for various dicarbon defect structures.

	Lattice mismatch (ppm)				
	Experimental	Calculated			
Sample	± 50	Only C_{As}	[100] $(CC)^+$	[110] $(CC)^+$	[111] $(CC)^+$
1	−450	−454			
2	≃160		−266	−207	−160
3	−1609	−1579			
4	−834		−1139	−1002	−891
5[a]	−1650		−1906	−1823	−1756
6[a]	−850		−1328	−1066	−853
7	−2311	−2332			
8	−1266		−1690	−1491	−1329

[a]The experimental data are from samples grown by MOVPE reported by Hanna and Mayerfeld (Ref. 2).

Our results, which suggest the dicarbon defects in compensated GaAs:C layers are dominated by the $[111]\text{-}(CC)^+$ structure, are consistent with the Raman spectra of the dicarbon defect.[9] In the Raman spectra, two peaks that are related to the dicarbon defects are located at 1742 and 1859 cm^{-1}, respectively. The fact that the intensity of the major peak at 1742 cm^{-1} is greater than that of the minor peak at 1859 cm^{-1} indicates that a single domineering type of dicarbon structure in the compensated GaAs:C epitaxial layer is present, in agreement with our results. Hence, this suggests that the major Raman peak at 1742 cm^{-1} may be attributed to the $[111]\text{-}(CC)^+$ structure. Due to the fact that the 1742 and 1859 cm^{-1} peaks were observed simultaneously, the difference in configuration energy between the structure attributed to the 1742- and 1859-cm^{-1} peaks, respectively, cannot be significantly greater than 0.025 eV.[10] Since the configuration energy of the $[100]\text{-}(CC)^+$ structure is 0.5-eV greater than that of the $[111]\text{-}(CC)^+$ structure, the 1859-cm^{-1} peak cannot be attributed to the $[100]\text{-}(CC)^+$ structure.[10] On the other hand, the configuration energy of the $[110]\text{-}(CC)^+$ structure is indistinguishable from that of the $[111]\text{-}(CC)^+$ structure[10] and our results, which merely suggest the dominance of the $[111]\text{-}(CC)^+$ structure, do not rule out the existence of the $[110]\text{-}(CC)^+$ structure in insignificant quantities, as stated earlier. Therefore, it is suggested that the 1859-cm^{-1} peak may be attributed to the $[110]\text{-}(CC)^+$ structure. The $[110]\text{-}(CC)^+$ structure can be formed either during annealing or high-temperature growth along with the $[111]\text{-}(CC)^+$ structure, or formed during Raman-scattering measurements.

V. CONCLUSION

This paper reports an investigation of dicarbon defects in a compensated GaAs:C epitaxial layer based on theoretical calculations, in conjunction with Hall effect, SIMS, and XRD lattice mismatch data. The GaAs:C layers were doped using C from a CBR_4 source in solid source MBE. The results strongly suggest the dicarbon defects in the compensated GaAs:C epitaxial layer mainly take the form of the $[111]\text{-}(CC)^+$ structure. Relating these results to the presence of the 1742- and 1859-cm^{-1} peaks in the Raman spectra suggests that the 1742- and 1859-cm^{-1} peaks can be attributed to the $[111]\text{-}(CC)^+$ and $[110]\text{-}(CC)^+$ structures, respectively.

[1] N. Kobayashi, T. Makimoto, and Y. Horikoshi, Appl. Phys. Lett. **50**, 1435 (1987).

[2] M. C. Hanna and A. Majerfeld, Appl. Phys. Lett. **59**, 2001 (1991).

[3] D. Lubyshev, M. Micovic, N. Gratteau, W. Z. Cai, D. L. Miller, O. Ray, R. W. Streater, and A. J. Spring Thorpe, J. Vac. Sci. Technol. B **17**, 1180 (1999).

[4] B. R. Davidson, R. C. Newman, T. J. Bullough, and T. B. Joyce, Phys. Rev. B **48**, 17 106 (1993).

[5] K. Woodhouse, R. C. Newman, T. B. Joyce, J. M. Woodall, G. J. Scilla, and F. Cordone, Semicond. Sci. Technol. **6**, 330 (1991).

[6] L. Hart, B. R. Davidson, J. M. Fernández, R. C. Newman, and C. C. Button, Mater. Sci. Forum **196–201**, 409 (1995).

[7] S. P. Westwater, and T. J. Bullough, J. Cryst. Growth **170**, 752 (1997).

[8] B. Cheong, and K. J. Chang, Phys. Rev. B **49**, 17 436 (1994).

[9] J. Wagner, R. C. Newman, B. R. Davidson, S. P. Westwater, T. J. Bullough, T. B. Joyce, C. D. Latham, R. Jones, and S. Öberg, Phys. Rev. Lett. **78**, 74 (1997).

[10] B. R. Davidson, R. C. Newman, C. D. Latham, R. Jones, J. Wagner, C. C. Button, and P. R. Briddon, Phys. Rev. B **60**, 5447 (1999).

[11] W. E. Hoke, D. G. Weir, P. J. Lemonias, and H. T. Hendriks, Appl. Phys. Lett. **64**, 202 (1994).

[12] V. Swaminathan and A. T. Macrander, *Material Aspects of GaAs and InP Based Structures* (Prentice-Hall, Englewood Cliffs, NJ, 1991), p. 191.

[13] N. Chen, Y. Wang, H. He, and L. Lin, Phys. Rev. B **54**, 8516 (1996).

[14] W. K. Liu, D. I. Lubyshev, P. Specht, R. Zhao, E. R. Weber, J. Gebauer, A. J. SpringThorpe, R. W. Streater, S. Vijarnwannaluk, W. Songprakob, and R. Zallen, J. Vac. Sci. Technol. B **18**, 1594 (2000).

[15] T. Kitatani, M. Kondow, and T. Tanaka, J. Cryst. Growth **227–228**, 521 (2001).

[16] J. Wagner, M. Maier, Th. Lauterbach, K. H. Bachem, A. Fischer, K. Ploog, G. Mörsch, and M. Kamp, Phys. Rev. B **45**, 9120 (1992).